Four p53 DNA-binding domain peptides bind natural p53-response elements and bend the DNA

(cooperative DNA binding/DNA bending/cyclization)

Pichumani Balagurumoorthy*, Hiroshi Sakamoto†, Marc S. Lewis‡, Nicola Zambrano†,
G. Marius Clore§, Angela M. Gronenborn§, Ettore Appella†, and Rodney E. Harrington*¶

*Department of Biochemistry, University of Nevada Reno, Reno, NV 89557-0014; and †Laboratory of Cell Biology, Building 37, National Cancer Institute,
‡Biomedical Engineering and Instrumentation Program, National Center for Research Resources, and §Laboratory of Chemical Physics, Building 5,
National Institute of Diabetes and Digestive and Kidney Diseases, National Institutes of Health, Bethesda, MD 20892

ABSTRACT   Recent structural studies of the minimal core DNA-binding domain of p53 (p53DBD) complexed to a single consensus pentamer sequence and of the isolated p53 tetramerization domain have provided valuable insights into their functions, but many questions about their interacting roles and synergism remain unanswered. To better understand these relationships, we have examined the binding of the p53DBD to two biologically important full-response elements (the WAF1 and ribosomal gene cluster sites) by using DNA circularization and analytical ultracentrifugation. We show that the p53DBD binds DNA strongly and cooperatively with p53DBD to DNA binding stoichiometries of 4:1. For the WAF1 element, the mean apparent K_d is $(8.3 \pm 1.4) \times 10^{-8}$ M, and no intermediate species of lower stoichiometries can be detected. We show further that complex formation induces an axial bend of at least 60° in both response elements. These results, taken collectively, demonstrate that p53DBD possesses the ability to direct the formation of a tight nucleoprotein complex having the same 4:1 DNA-binding stoichiometry as wild-type p53 which is accompanied by a substantial conformational change in the response-element DNA. This suggests that the p53DBD may play a role in the tetramerization function of p53. A possible role in this regard is proposed.

Wild-type p53 is a 53-kDa nuclear phosphoprotein that occurs in a wide variety of organisms. Its role as a tumor suppressor is well documented, and its inactivation, either through mutation or interaction with cellular or viral proteins, is strongly correlated with human cancer (1–3). Virtually all of the presently known biological functions of p53 depend critically upon its DNA-binding properties (4–6). Much of the evidence for this is based upon its role as an enhancer (7) and transcription factor (4, 5, 8) for genes that mediate growth arrest and DNA-damage repair through their gene products, including WAF1 which codes for a protein that inhibits several cyclin-dependent protein kinases necessary for cell cycle progression from G_1 into S (9). The many regulatory roles for p53 and its large variety of binding sites suggest that its specificity of binding to individual DNA binding sites holds an important clue to its function in its interactions with other regulatory proteins (10).

Wild-type p53 may bind to over 100 different naturally occurring DNA binding sites or response elements, and the human genome may contain between 200 and 300 such sites (11). Most of the functional response elements contain two tandem decameric elements, each a pentameric inverted repeat. Most decamers follow the consensus sequence pattern PuPuPuC(A/T)|(A/T)GPyPyPy (11, 12), where Pu and Py are purines and pyrimidines, respectively, and the vertical bar

indicates the center of dyad symmetry. Response elements are bound by a well-defined central region of the p53 protein, the core DNA-binding domain of p53 (p53DBD), amino acids 96–308. A tetramerization domain extending from amino acid 319 to 360 is thought to be responsible for the tetrameric state of wild-type p53 both free in solution and bound to its specific DNA binding sites (7, 13, 14). Tetramerization has been proposed to play a major part in wild-type p53 function by modulating its DNA-binding properties (15, 16) and by influencing its role as a transcriptional enhancer and activator through DNA looping (7). Crystallographic (17) and NMR (15, 16, 18) structures for the tetramerization domain have recently become available.

A cocrystal structure has recently been reported for p53DBD bound to a half response element (19). This structure provides much insight into the binding specificity by identifying specific binding contacts but cannot address possible intermolecular interactions among bound peptides or provide direct information on the nature of the tetrameric complex. In this work, we address these questions by examining the binding of p53DBD with two, full, biologically important response elements from the WAF1 gene and the ribosomal gene cluster (RGC). Using T4 ligase-mediated cyclization, gel band-shift assays, and analytical ultracentrifugation, we show that p53DBD binds cooperatively to the full response element as a tetrapeptide and induces substantial bending in the response-element DNA. Although many transcription factors are known to bend their DNA binding sites (20–22), this type of bending has not been reported previously for p53DBD. Although p53DBD exists under most conditions as a monomer free in solution (23, 24), the present findings show that it possesses a remarkable self-organizing ability upon DNA binding, including the capacity to alter the DNA structure. This may maximize binding stereospecificity and affinity through tetrapeptide formation, and, hence, p53DBD appears to play an important role in the overall tetramerization property of p53.

MATERIALS AND METHODS

Preparation of the p53DBD Peptide. A portion of the human p53 cDNA encoding amino acid residues 96–308 was amplified by PCR by using p53-specific primers 5'-ATATCATATGG-TCCCTTCCCAGAAAACCTA-3' and 5'-ATATGGATCC-TCACAGTGCTCGCTTAGTGCTC-3'. The amplified product was inserted in the pET12a expression vector (Novagen), and the core DNA-binding domain was produced in *Escherichia coli* BL21 (DE3). The cells were incubated at 37°C until they reached an OD_{600} of 0.6–1.0, and 0.25 mM isopropyl β-D-thiogalactoside (IPTG) was added to induce the expres-

Abbreviations: p53DBD, DNA-binding domain of p53; RGC, ribosomal gene cluster; DTT, dithiothreitol.
¶To whom reprint requests should be addressed.

sion of the recombinant protein. Cells were harvested 2 h later by centrifugation, lysed in French press, and sonicated for 2 min in 40 mM Mes, pH 6.0, 100 mM NaCl/5 mM dithiothreitol (DTT). The soluble fraction was loaded onto a Resource S column (Pharmacia) in 40 mM Mes, pH 6.0/5 mM DTT, and was eluted by a 0–400 mM NaCl gradient. The pooled fractions were precipitated by addition of ammonium sulfate to 80% saturation and purified further on a Superdex 75 HR gel-filtration column (Pharmacia) in 50 mM Bis-Tris propane·HCl, pH 6.8/100 mM NaCl/1 mM DTT. The purified p53DBD ran as a single band on an SDS/polyacrylamide gel.

Determination of Binding Stoichiometries. Binding stoichiometries of p53DBD to the response-element duplexes (Fig. 1) were determined by using standard band-shift assays (29, 30). Various amounts of p53DBD were incubated with a fixed amount of 5′ end-labeled duplex of known concentration in 50 mM Bis-Tris propane·HCl, pH 6.8, containing 10 mM $MgCl_2$ and 10 mM DTT in a total volume of 10 μl on ice for 45 min, electrophoresed through a 4% nondenaturing polyacrylamide gel in 0.3× TBE (1× TBE = 89 mM Tris·HCl/89 mM boric acid/2 mM EDTA). Identical unbound response-element DNA controls were run in parallel. After autoradiography, the free, unbound DNA and p53DBD–DNA complex bands were excised, the amount of radioactivity contained in them was counted, and the amount of DNA in the complex was calculated as the difference between counts for total DNA and that remaining in the free DNA band. The excised DNA–protein complex bands were then soaked in SDS-containing stacking gel buffer for 5 min, fractionated on a SDS/12.5% polyacrylamide gel, which was stained with Coomassie blue. The Coomassie blue in the stained band was eluted with 25% (vol/vol) pyridine in water overnight, and the absorbance was measured at 605 nm at 25°C. Unbound p53DBD did not comigrate with the complex, as shown by comparison of stained gels with autoradiographs taken from them (data not shown). As controls, the same amounts of protein used in the binding reactions were electrophoresed through an SDS/12.5% polyacrylamide gel, the gel was stained with Coomassie blue, and the dye absorbance was measured for quantitation. From this, the amount of p53DBD associated with the protein–DNA complex was estimated.

Determination of Binding Affinities by Using Analytical Ultracentrifugation. The molar concentration distributions in the ultracentrifugation studies were obtained by using the multiwavelength scanning technique, which permits transformation of absorbancies as functions of radial position at different wavelengths into the total molar concentrations of each component as a function of radial position (31, 32). The equilibrium concentration gradients of nucleic acid and protein were fit with appropriate functions for a 4:1 protein to DNA stoichiometry as follows:

$$C_{r,T,N} = C_{b,N}\exp[A_N M_N(r^2 - r_b^2)] + C_{b,N}C_{b,P}^4\exp[\ln K_{14}$$
$$+ (A_N M_N + 4A_P M_P)(r^2 - r_b^2)]$$

and

$$C_{r,T,P} = C_{b,P}\exp[A_P M_P(r^2 - r_b^2)] + 4C_{b,N}C_{b,P}^4\exp[\ln K_{14}$$
$$+ A_N M_N + 4A_P M_P)(r^2 - r_b^2)],$$

where K_{14} is the overall equilibrium association constant for the complex; $C_{r,T,N}$ and $C_{r,T,P}$ are the total molar concentrations (uncomplexed plus complexed) of DNA and peptide, respectively; the C_b and M variables are respectively the uncomplexed concentrations of each component at the reference position of the cell bottom (r_b) and the molecular masses (M_N = 12384 Da, M_P = 23932 Da); and $A = (\partial\rho/\partial c)_\mu\omega^2/2RT[(\partial\rho/\partial c)_\mu$, the density increment at constant chemical potential, is obtained experimentally for each component in the ultracentrifuge; ω is the rotor angular velocity; R is the gas constant; and T is the absolute temperature]. The two data sets were fit simultaneously with these equations, optimizing $\ln K_{14}$ as a global parameter, and $C_{b,N}$ and $C_{b,P}$ as local parameters, with a joint fit rms error of 0.0457 μM.

Measurement of DNA Bending. DNA bending was determined by T4 DNA ligase-mediated cyclization by using methods similar to those described previously (27, 28, 33). The response-element duplexes (Fig. 1) were kinased with [γ-^{32}P]-ATP and unlabeled ATP. In cyclization experiments, 1.5 μg of the 5′ phosphorylated response-element duplex in 10 μl of 50 mM NaCl was incubated with 25 μl of p53DBD (1.32 μg/μl) in 50 mM Bis-Tris propane·HCl, pH 6.8/100 mM NaCl/1 mM DTT for 45 min on ice, and ligations were carried out for 16 h at 4°C. Control experiments without p53DBD were done in parallel at the same DNA concentration under identical conditions to normalize any DNA concentration effects on microcircle formation. The reaction was arrested with SDS and EDTA, and the solution was extracted three times with phenol and twice with a chloroform/isoamyl alcohol (24:1) mixture. The DNA was precipitated with ethanol and analyzed by a two-dimensional/electrophoresis assay, with 5% nondenaturing polyacrylamide gels in the first dimension and run on an 8% nondenaturing polyacrylamide second dimension containing 50 μg/ml of chloroquine. The gel was then autoradiographed. Covalently closed microcircles (Fig. 4) were eluted from the gel and analyzed on denaturing gels as described (27). These procedures preclude misidentification of possible looped structures as microcircles since loops resulting from the simultaneous binding of p53DBD to multiple response elements in linearly ligated precursor fragments similar to that described for intact p53 protein (7) would be lost when the bound peptides are removed prior to electrophoresis.

```
5′  TCATCAGGAACATGTCCCAACATGTTGAGCTC 3′
    ||||||||||||||||||||||||||||||||
 3′  AGTCCTTGTACAGGGTTGTACAACTCGAGAGT 5′
     |<------------------->|
            20 nt WAF1 site


5′  TCCGATTGCCTTGCCTGGACTTGCCTGGCCTT 3′
    ||||||||||||||||||||||||||||||||
 3′  CTAACGGAACGGACCTGAACGGACCGGAAAGG 5′
     |<------------------->|
            20 nt RGC site
```
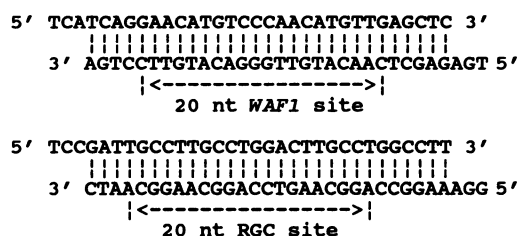
FIG. 1. Precursor oligomers used for studies reported in this work. The 20-nt response elements for the *WAF1* site (25, 26) and the RGC site (23, 24) were incorporated into 32-nt synthetic oligonucleotides so that, when ligated, each binding site was located roughly in the center of a double-stranded sequence of precisely three helical repeats. The 3-nt overhanging ends assure efficient head-to-tail ligation (cyclization) for oligomers having correct fixed curvature and proper torsional and axial end alignment (27, 28).

RESULTS

p53DBD Binds *WAF1* and RGC Response Elements Cooperatively and with a 4:1 Peptide to DNA Stoichiometry. The binding stoichiometry of the p53DBD to the two response elements was established by two methods: (*i*) quantitation of the amount of p53DBD and DNA present in the complex in band-shift assays (Fig. 2*A*) and (*ii*) quantitation by analytical ultracentrifugation (Fig. 3). Both methods yield a stoichiometry of four p53DBD peptides to one response element for both *WAF1* and RGC response elements. Least squares analysis of the analytical ultracentrifugation data in Fig. 3 gives a value of $\ln K_{14}$ of 65.17 ± 0.69 at 20°C. This corresponds to an overall dissociation constant of 4.98 × 10^{-29} M^4 and a binding free energy of −37.9 kcal·mol^{-4}.

As shown in Fig. 3, attempts to fit the data with models corresponding to a 1:1 or 2:1 peptide to DNA stoichiometry

Biochemistry: Balagurumoorthy *et al.*

Proc. Natl. Acad. Sci. USA 92 (1995) 8593
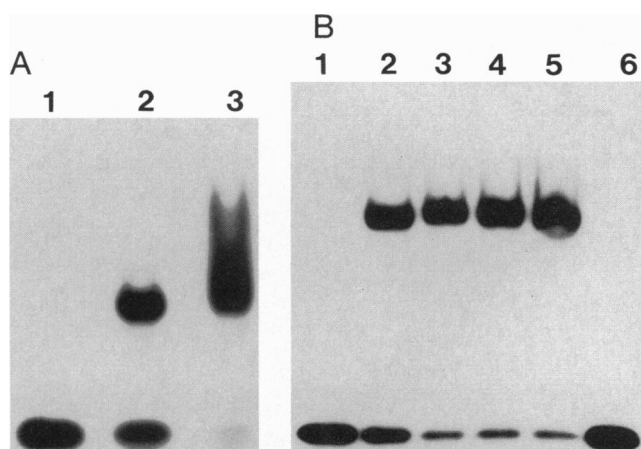
FIG. 2. Band-shift assays for determining stoichiometry and demonstrating cooperativity for p53DBD binding to the *WAF1* response element. Similar results were obtained for the RGC response element (data not shown). (*A*) Band-shift assay for determining the stoichiometries of the *WAF1* response element complexed with p53DBD. Numerical values given below apply to the *WAF1* response element; similar values were obtained for the RGC response element. All three lanes contain the same amount of DNA carrying equal amounts of radiolabel (26.4×10^{-12} mol). Lane 1, response element duplex alone; lane 2, response element duplex plus 1 μl of p53DBD (55.2×10^{-12} mol); and lane 3, response element duplex plus 2 μl of p53DBD (110×10^{-12} mol). The amount of DNA associated with p53DBD–DNA complexes in lanes 2 (12.0×10^{-12} mol) and 3 (24.0×10^{-12} mol) was determined by scintillation counting and comparing the free DNA bands in lanes 2 and 3 with that of lane 1. The amount of p53DBD in the p53DBD–DNA complex was estimated as described in the text. Lanes 2 and 3 contain 49.3×10^{-12} and 99.2×10^{-12} mol of p53DBD, respectively, corresponding to a binding stoichiometry of 4.12:1 for the p53DBD–*WAF1* response element complex. (*B*) Electrophoretic mobility-shift assay used to demonstrate the cooperative binding of the p53DBD to the *WAF1* duplex. A total of 5 ng of ^{32}P-labeled *WAF1* duplex was incubated with various amounts of p53DBD in a 10-μl volume containing 50 mM Bis-Tris propane·HCl, pH 6.8/100 mM NaCl/1 mM DTT for 40 min on ice. A total of 2 μl of 50% glycerol was added, and the samples were analyzed on a nondenaturing 5% polyacrylamide gel, as described in the text. Amounts of p53DBD peptide used were as follows: lane 1, 108 ng; lane 2, 216 ng; lane 3, 324 ng; lane 4, 432 ng; lane 5, 540 ng; and lane 6, control with no added p53DBD.

fail. Stepwise equilibrium models are also ruled out since the concentrations of species other than free peptide, free DNA, and the 4:1 complex are too low to be observable. Thus, the binding of four molecules of p53DBD to each response element occurs in a highly cooperative manner to form a nucleoprotein complex in which the bound p53DBD peptides are in very close and precise juxtaposition. A similar lack of intermediate species apparent in Fig. 2*B* provides additional evidence for binding cooperativity. Under these circumstances, the cooperativity parameter cannot be determined, and the mean apparent equilibrium dissociation constant per p53DBD monomer (which incorporates the cooperativity parameter) is obtained from the ultracentrifugation results as $(8.3 \pm 1.4) \times 10^{-8}$ M.

p53DBD Tetrapeptide Binding to the *WAF1* and RGC Sites Bends the Response Element DNA. Clear evidence for DNA bending in the tetrapeptide complexes between p53DBD and the *WAF1* and RGC response elements has been obtained from T4 DNA ligase mediated cyclization studies (Fig. 4). Cyclization or ring closure is a powerful and unambiguous method of demonstrating curvature in protein–DNA complexes (27, 28, 33, 34). Recent studies on the binding of the λ phage Cro protein by using the present methods (27) have been corroborated by direct imaging with scanning force microscopy (35).
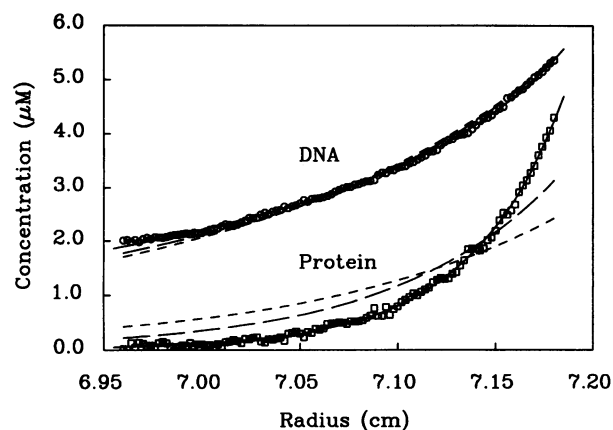
FIG. 3. Total molar concentrations of *WAF1* (free and complexed, ○) and p53 DNA-binding domain (free and complexed, □) as a function of radial position at centrifugal and chemical equilibrium at 20°C and 16,000 rpm in a Beckman XL-A analytical ultracentrifuge. These data are fit with mathematical models for a 4:1 p53DBD to *WAF1* stoichiometry (solid lines), 2:1 stoichiometry (long-dashed lines), and 1:1 stoichiometry (short-dashed lines). It is readily apparent that only a model based upon 4:1 stoichiometry is appropriate.

Second dimension gels for p53DBD bound to the precursor oligonucleotides shown in Fig. 1 are given in Fig. 4*A* and *B* for *WAF1* and RGC, respectively. Fig. 4 *C* and *D* shows the respective free-DNA controls. Topologically relaxed, covalently closed microcircles appear as the second row of spots from the top in each figure. Correspondingly sized nicked microcircles appear just above these, and linear species appear on the diagonal. Each of the two response elements bound to p53DBD gives essentially similar patterns (Fig. 4*A* and *B*), and the smallest microcircles that appear with full intensity correspond to hexamers of the 32-bp precursor oligonucleotides (192 bp). This suggests that each bound response element has a minimum absolute bending angle of $\approx 60°$, defined as the angular difference between tangents to the two arms in the bent conformation (27, 28). Control experiments in the absence of p53DBD show no microcircles for the *WAF1*-response element (Fig. 4*C*) and only weak spots for the RGC-response element (Fig. 4*D*). Thus, essentially all curvature must originate in the peptide-bound response elements.

The weak appearance of relatively large microcircles in the free-DNA controls for the RGC site may be associated with the run of five half-helically phased TG·CA sequence elements, as these chiefly differentiate the RGC sequence from the *WAF1* sequence, which showed no evidence for cyclization in the control (Fig. 4*C*). Computer modeling (22) showed no tendency for this sequence to cyclize as observed in Fig. 4*D* unless hinge kinking was permitted with variable roll in both the positive (into the major groove) and negative (into the minor groove) sense in each TG·CA element. In this case, almost perfect end alignments were obtained for the RGC site-containing sequence, whereas the *WAF1* sequence showed similar circularity but with a small but significant superhelical writhe. These results suggest that DNA flexibility may be an important attribute of p53-response elements. Alternatively, it is possible that differences in intrinsic bending may differentiate these two response elements since the *WAF1* element contains helically phased AA·TT dinucleotides.

The estimate of $\approx 60°$ for DNA bending angles is undoubtedly a lower limit value. The bending angles in these studies may be limited by steric restrictions imposed by the bound protein since we do not observe circular spots smaller than $6 \times 32 = 192$ bp for either of the peptide-bound systems (Fig. 4 *A* and *C*). These 192-bp circular spots appear with relatively high spot intensities, and yet the larger circle size spots in Fig. 4 *A* and *C* have a distribution of intensities that corresponds to
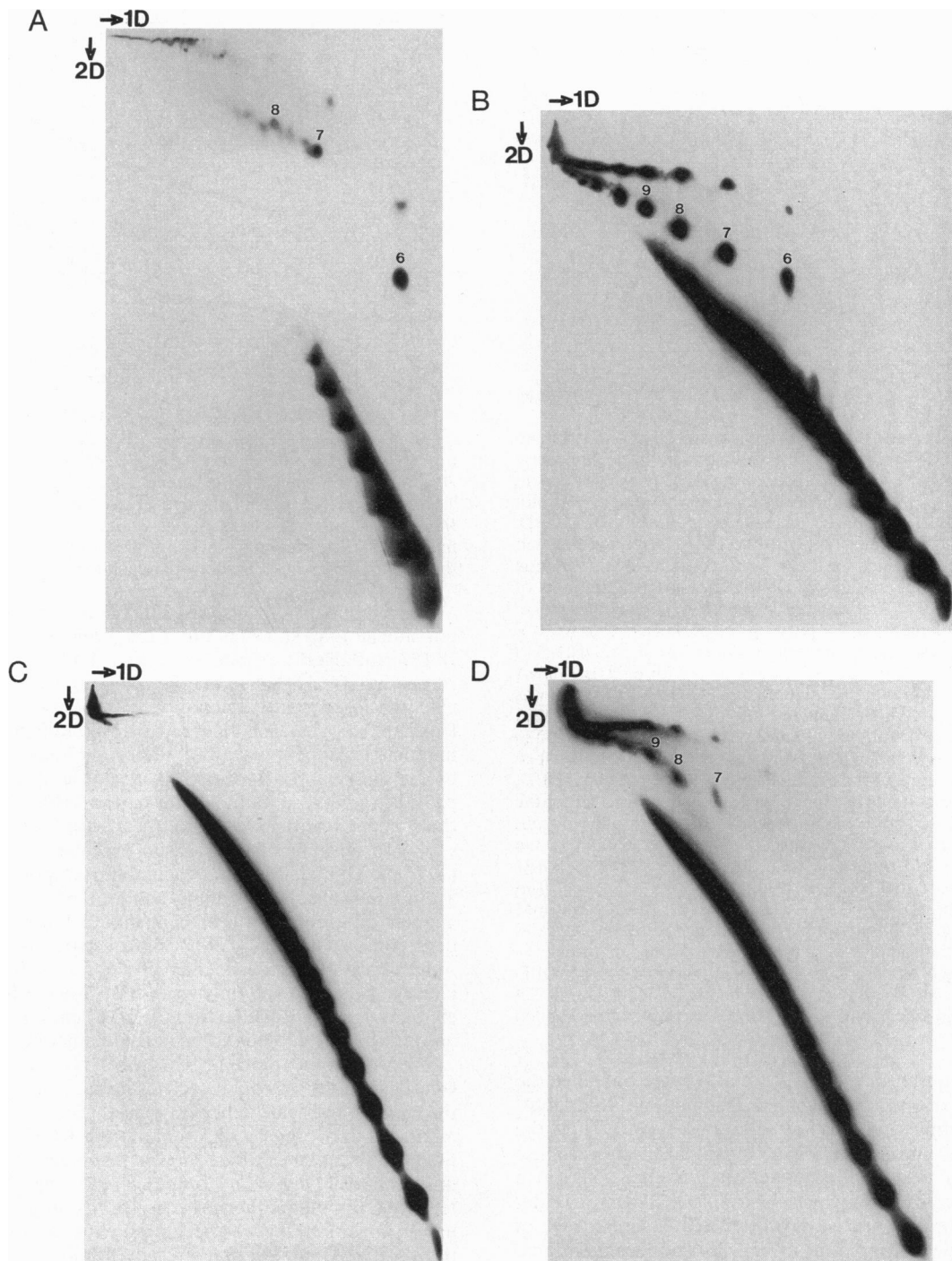
FIG. 4.   Two-dimensional polyacrylamide gel electrophoresis assays for the analysis of ligation products of the precursor duplexes shown in Fig. 1 in the presence (*A* and *B*) and absence (*C* and *D*) of p53DBD. (*A* and *C*) *WAF1*; (*B* and *D*) RGC. The upper row of spots corresponds to nicked microcircles, the central row to covalently closed microcircles, and linear species lie on the diagonal. Closed circle sizes, as indicated, were determined by analyzing the DNA from the respective spots on denaturing gels with *Hpa* II-digested ^{32}P-labeled pBR322 fragments as size markers. 1D, first dimension; 2D, second dimension.

the larger circle-size portion of the thermal-intensity distribution normally observed with pure DNA—e.g., Fig. 4*D*—and with DNA bound by smaller proteins (27, 28). This suggests that the intensity distributions are cut off at a ring size of 192 bp, presumably by steric restrictions. Steric restrictions appear to account for discrepancies between bending angles obtained by using the present methods for the λ phage Cro protein bound to an operator site (27) and those obtained by direct imaging with scanning force microscopy (35). Thus, the actual bending angles may be considerably greater than 60° since

p53DBD has almost twice the molecular weight of the Cro protein. However, the fact that microcircles are observed for both the *WAF1* and RGC sites is an unambiguous reflection of curvature in the 32-bp precursor oligomers beyond that due to the DNA alone. Out-of-plane writhe induced in the bound precursors generally leads to no microcircle formation, and torsional or angular mismatch of the single strand ends can seriously reduce it. The latter two may affect the distribution of spot intensities with circle sizes since they are cumulative with ligation. Strong microcircle formation also suggests that

the complexes form with little change in overall DNA winding since the precursor sequences, before complex formation, have integral helical repeat by design. This is clearly the case for the bound RGC site (Fig. 4*B*), which has a typically thermal distribution of circular spot intensities. The distribution for the *WAF1* site (Fig. 4*A*) suggests that the bound peptides may induce a small writhe or overall winding distortion in the DNA, but any such distortion must be small because of the relatively high intensity of the $6 \times 32 = 192$ bp spot in Fig. 4*A*.

DISCUSSION

Based on the cocrystal structure of p53DBD bound to a single consensus binding-site pentamer, Cho *et al.* (19) proposed a model for the binding of four p53DBD peptides to a full 20-bp p53-response element that showed that binding of four interacting p53DBD peptides to such a site can occur without steric clash. While the model was proposed for straight DNA, it does not preclude DNA bending. Indeed, the net effect of DNA bending would be to bring the four bound p53DBD peptides into closer juxtaposition and maximize potential protein–protein interactions within the complex. The locus of bending cannot be determined from these experiments but may arise from putative flexibility elements such as CA·TG (22) and GGGC·GCCC (36), which are represented not only in the *WAF1* and RGC response elements investigated here but are common features in most p53-binding sites (11, 25).

Our finding that four p53DBD peptides interact with p53-response elements is in agreement with the recent mixing experiments of Wang *et al.* (37). However, our observation that four p53DBD peptides can direct the formation of tight-association complexes which bend the binding-site DNA has a number of additional interesting ramifications. (*i*) Bent DNA in the complex may facilitate mechanisms by which efficient binding can occur to p53-response elements whose palindromic decameric elements are separated by neutral spacers, since separations as great as 13 bp (12) and even 21 bp (38) have been reported in response elements with high affinity for p53 binding. (*ii*) DNA bending by p53 may serve an architectural role in bringing together other protein factors bound to either side of the p53 site (39). (*iii*) Since p53DBD evidently associates only when binding to response-element DNA, it is possible that it undergoes allosteric conformational changes as it forms a tetrapeptide complex. Evidence for allosteric regulation of DNA binding in wild-type p53 is already available (7, 38, 40, 41). (*iv*) An important function for the p53-tetramerization domain may be to direct the association of p53 monomers, thereby providing both a higher level of control and a strengthening of DNA binding. In this regard, it should be noted that the binding of intact p53 [estimated as $K_d \approx 6 \times 10^{-9}$ M for the RGC site (42) and $K_d \approx 5 \times 10^{-10}$ M for the consensus p53-CON site (43)] is 10- to 100-fold higher than that of the p53DBD [apparent $K_d = (8.3 \pm 1.4) \times 10^{-8}$ M for the *WAF1* site from this work]. Although binding differences are to be expected among different response elements (42), this binding enhancement by the intact protein is substantial. A possible explanation for this phenomenon is that tetramerization of p53 reduces the entropy of the free state and, hence, the entropy difference between the free and bound states.

1. Hollstein, M., Sidransky, D., Vogelstein, B. & Harris, C. C. (1991) *Science* 253, 49–53.
2. Lane, D. P. (1992) *Nature (London)* 358, 15–16.
3. Levine, A. J. (1993) *Annu. Rev. Biochem.* 62, 623–651.
4. Prives, C. (1994) *Cell* 78, 543–546.
5. Milner, J. (1994) *Semin. Cancer Biol.* 5, 211–219.
6. Anderson, M. E. & Tegtmeyer, P. (1995) *BioEssays* 17, 3–7.
7. Stenger, J. E., Tegtmeyer, P., Mayr, G. A., Reed, M., Wang, Y., Wang, P., Hough, P. V. C. & Mastrangelo, I. A. (1994) *EMBO J.* 13, 6011–6020.
8. Prives, C. & Manfredi, J. J. (1993) *Genes Dev.* 7, 529–534.
9. Hartwell, L. H. & Kastan, M. B. (1994) *Science* 266, 1821–1828.
10. Appella, E. & Anderson, C. W. (1994) *Biochim. Italia* 1, 19–28.
11. Tokino, T., Thiagalingam, S., El-Deiry, W. S., Waldman, T., Kinzler, K. W. & Vogelstein, B. (1994) *Hum. Mol. Genet.* 3, 1537–1542.
12. El-Deiry, W. S., Kern, S. E., Pietenpol, J. A., Kinzler, K. W. & Vogelstein, B. (1992) *Nature Genet.* 1, 45–49.
13. Friedman, P. N., Chen, X. B., Bargonetti, J. & Prives, C. (1993) *Proc. Natl. Acad. Sci. USA* 90, 3319–3323.
14. Sakamoto, H., Lewis, M. S., Kodama, H., Appella, E. & Sakaguchi, K. (1994) *Proc. Natl. Acad. Sci. USA* 91, 8974–8978.
15. Clore, G. M., Omichinski, J. G., Sakaguchi, K., Zambrano, N., Sakamoto, H., Appella, E. & Gronenborn, A. M. (1994) *Science* 265, 386–391.
16. Lee, W., Harveyo, T. S., Yin, Y., Yau, P., Litchfield, D. & Arrowsmith, C. H. (1994) *Nature (London) Struct. Biol.* 1, 877–890.
17. Jeffrey, P. D., Gorina, S. & Pavletich, N. P. (1995) *Science* 267, 1498–1502.
18. Clore, G. M., Omichinski, J. G., Sakaguchi, K., Zambrano, N., Sakamoto, H., Appella, E. & Gronenborn, A. M. (1995) *Science* 267, 1515–1516.
19. Cho, Y. J., Gorina, S., Jeffrey, P. D. & Pavletich, N. P. (1994) *Science* 265, 346–355.
20. Steitz, T. A. (1990) *Q. Rev. Biophys.* 23, 205–280.
21. Harrington, R. E. (1992) *Mol. Microbiol.* 6, 2549–2555.
22. Harrington, R. E. & Winicov, I. (1994) in *Progress in Nucleic Acids Research and Molecular Biology*, eds. Cohn, W. & Moldave, K. (Academic, San Diego), Vol. 47, pp. 195–270.
23. Pavletich, N. P., Chambers, K. A. & Pabo, C. O. (1993) *Genes Dev.* 7, 2556–2564.
24. Greenblatt, M. S., Bennett, W. P., Hollstein, M. & Harris, C. C. (1994) *Cancer Res.* 54, 4855–4878.
25. Funk, W. D., Pak, D. T., Karas, R. H., Wright, W. E. & Shay, J. W. (1992) *Mol. Cell. Biol.* 12, 2866–2871.
26. El-Deiry, W. S., Tokino, T., Velculescu, V. E., Levy, D. B., Parsons, R., Trent, J. M., Lin, D., Mercer, W. E., Kinzler, K. W. & Vogelstein, B. (1993) *Cell* 75, 817–825.
27. Lyubchenko, Y. L., Shlyakhtenko, L. S., Chernov, B. & Harrington, R. E. (1991) *Proc. Natl. Acad. Sci. USA* 88, 5331–5334.
28. Harrington, R. E. (1993) *Electrophoresis* 14, 732–746.
29. Garner, M. M. & Revzin, A. (1990) in *Gel Electrophoresis of Nucleic Acids: A Practical Approach*, eds. Rickwood, D. & Hames, B. D. (IRL, New York), pp. 201–223.
30. Hames, B. D. (1990) in *Gel Electrophoresis of Proteins: A Practical Approach*, eds. Rickwood, D. & Hames, B. D. (IRL, New York), pp. 1–91.
31. Lewis, M. S., Shrager, R. I. & Kim, S.-J. (1994) in *Modern Analytical Ultracentrifugation*, eds. Schuster, T. M. & Laue, T. M. (Birkhaeuser, Boston), pp. 94–118.
32. Kim, S. J., Tsukiyama, T., Lewis, M. S. & Wu, C. (1994) *Protein Sci.* 3, 1040–1051.
33. Zahn, K. & Blattner, F. R. (1987) *Science* 236, 416–422.
34. Kahn, J. D. & Crothers, D. M. (1992) *Proc. Natl. Acad. Sci. USA* 89, 6343–6347.
35. Erie, D. A., Yang, G. L., Schultz, H. C. & Bustamante, C. (1994) *Science* 266, 1562–1566.
36. Brukner, I., Susic, S., Dlakic, M., Savic, A. & Pongor, S. (1994) *J. Mol. Biol.* 236, 26–32.
37. Wang, Y., Schwedes, J. F., Parks, D., Mann, K. & Tegtmeyer, P. (1995) *Mol. Cell. Biol.* 15, 2157–2165.
38. Waterman, J. L. F., Shenk, J. L. & Halazonetis, T. D. (1995) *EMBO J.* 14, 512–519.
39. Tjian, R. & Maniatis, T. (1994) *Cell* 77, 5–8.
40. Halazonetis, T. D., Davis, L. J. & Kandil, A. N. (1993) *EMBO J.* 12, 1021–1028.
41. Halazonetis, T. D. & Kandil, A. N. (1993) *EMBO J.* 12, 5057–5064.
42. Bargonetti, J., Reynisdottir, I., Friedman, P. N. & Prives, C. (1992) *Genes Dev.* 6, 1886–1898.
43. Hall, A. R. & Milner, J. (1995) *Oncogene* 10, 561–567.